ELSEVIER

Chemistry & Biology 8 (2001) 1033–1049

Chemistry & Biology

www.elsevier.com/locate/chembiol

Research Paper

The inefficiency of incisions of ecteinascidin 743–DNA adducts by the UvrABC nuclease and the unique structural feature of the DNA adducts can be used to explain the repair-dependent toxicities of this antitumor agent

Maha Zewail-Foote [a], Ven-Shun Li [b], Harold Kohn [b,1], David Bearss [c], Mary Guzman [c], Laurence H. Hurley [a,d,*]

[a] *Department of Chemistry and Biochemistry, The University of Texas at Austin, Austin, TX 78712, USA*
[b] *Department of Chemistry, University of Houston, Houston, TX 77204, USA*
[c] *Arizona Cancer Center, 1515 N. Campbell Avenue, Tucson, AZ 85724, USA*
[d] *College of Pharmacy, The University of Texas at Austin, Austin, TX 78712, USA*

Received 9 April 2001; revisions requested 8 June 2001; revisions received 10 July 2001; accepted 12 July 2001
First published online 12 September 2001

Abstract

Background: Ecteinascidin 743 (Et 743), a natural product derived from a marine tunicate, is a potent antitumor agent presently in phase II clinical trials. Et 743 binds in the minor groove of DNA and alkylates N2 of guanine via a unique mechanism involving catalytic activation. The sequence selectivity of Et 743 is governed by different patterns of hydrogen-bonding to DNA, which results in differential reversibility of the covalent adducts. As determined by nuclear magnetic resonance spectroscopy, the preferred sequences 5′-PuGC and 5′-PyGG are stabilized by a hydrogen-bonding network, while the non-preferred sequences 5′-NG(A/T) are much less stabilized due to the lack of a key hydrogen bond to the GC base pair on the 3′-side of the alkylated guanine.

Results: Mammalian cell lines (XPB, XPD, XPF, XPG, and ERCC1) deficient in the nucleotide excision repair (NER) gene products show resistance to Et 743. The recognition and subsequent incision of Et 743–DNA adducts by the bacterial multisubunit endonuclease UvrABC were used to evaluate DNA repair-mediated toxicity as a rationale for the resistance of NER-defective cell lines and the antitumor activity of Et 743. The Et 743–DNA adducts are indeed recognized and incised by the UvrABC repair proteins; however, the pattern of incision indicated that the non-preferred, and less stable, sequences (i.e. 5′-NG(A/T)) modified with Et 743 are generally incised at a much higher efficiency than the preferred, more stable sequences (i.e. 5′-PuGC or 5′-PyGG). In addition, within the same Et 743 recognition sequence, the level of incision varies, indicating that flanking regions also contribute to the differential incision frequency.

Conclusions: The inefficient repair incision by the UvrABC nuclease of Et 743–DNA adducts provides a basis for rationalizing the observed repair-dependent cytotoxicities of these DNA adducts, if other associated structural properties of Et 743–DNA adducts are taken into account. In particular, the wedge-shaped Et 743, which forces open the minor groove of DNA, introducing a major groove bend, and the extrahelical protrusion of the C-subunit of Et 743 provide unique characteristics alongside the hydrogen-bonding stabilization of a covalent DNA adduct, which we propose traps an intermediate in NER processing of Et 743–DNA adducts. This trapped intermediate protein–Et 743–DNA adduct complex can be considered analogous to a poisoned topoisomerase I– or topoisomerase II–DNA complex. In the absence of an intact NER nuclease complex, this toxic lesion is unable to form, and the Et 743–DNA adducts, although not

[1] Present address: Division of Medicinal Chemistry and Natural Products, University of North Carolina at Chapel Hill, Chapel Hill, NC 27599, USA.

* Corresponding author. Present addresses: The University of Arizona, Arizona Cancer Center, 1515 N. Campbell Avenue, Tucson, AZ 85724, USA, and The University of Arizona, College of Pharmacy, 1703 E. Mabel, Tucson, AZ 85721, USA.
E-mail address: hurley@pharmacy.arizona.edu (L.H. Hurley).

PII: S1074-5521(01)00071-0

repaired by the NER pathway, are less toxic to cells. Conversely, elevated levels of either of these nucleases should lead to enhanced Et 743 toxicity.

Keywords: Alkylating agent; Anticancer drug; DNA repair; Ecteinascidin

1. Introduction

The ecteinascidins (Ets) are extremely potent antitumor agents isolated from the marine tunicate *Ecteinascidia turbinata* [1]. Of the numerous Ets that have been isolated, Et 743 is the first to advance to clinical trials, where it is particularly active against soft tissue sarcomas [2–6]. Et 743 is a carbinolamine-containing antitumor agent composed of three fused tetrahydroisoquinoline rings and is structurally related to the DNA-reactive saframycins [7–9], naphthyridinomycin [10], and anthramycin [11] (Fig. 1A). The primary structural difference between the saframycins and Et 743 is that Et 743 contains an extra tetrahydroisoquinoline ring, the C-subunit, that is absent in this other antitumor antibiotic. While the A- and B-subunits of Et 743 provide the scaffold for DNA recognition and bonding, the C-subunit protrudes out of the minor groove, making only limited contacts with the DNA [12] (Fig. 2A). Like the other carbinolamine antibiotics, the Ets bond in the minor groove of DNA in a sequence-dependent manner and alkylate the N2 position of guanine [13]. Et 743–DNA adduct formation is mediated through an intramolecular acid-catalyzed dehydration of the carbinolamine moiety, resulting in an iminium intermediate that is the DNA-reactive species (Fig. 2B) [14].

Through gel mobility shift assays [13] and high-field nuclear magnetic resonance (NMR) studies [12,15], the preferred thermodynamic sequence of Et 743 has been shown to be 5′-PuG*C and 5′-PyG*G (* indicates the covalently modified guanine), while the non-preferred sequences are 5′-NG*(A/T). The Et 743–DNA hydrogen-bonding network that stabilizes the adduct is a major factor in determining sequence recognition. The formation of a hydrogen bond between one of the oxygens of the methylenedioxy ring of Et 743 and a proton in the exocyclic 2-amino group of the guanine located 3′ to the alkylated site on either strand (HB2 in Fig. 1B) largely determines if the bonding sequence yields a stable DNA adduct. Elimination of this hydrogen bond acceptor by replacing the 3′ G or C with an A or T makes the sequence less stable [16]. We have recently shown that the relative stabilities of the Et 743–DNA covalent adducts determine the rate of the Et 743–DNA covalent adduct reverse reaction, while the rate of the forward reaction is independent of the flanking sequence [16]. Hence, the sequence selectivity of Et 743 is determined by the relative kinetics of the covalent reversal reaction, which leads to the release of free Et 743 and rebonding at the same or different sequences (Fig. 2B). The net effect of this process is the time-dependent channeling of Et 743 to a subset of DNA sequences in which the Et 743–DNA adducts are thermodynamically stable. Thus, during a 6-h incubation, 20% of the initial covalent adduct at the less stable sequence migrates to the stable sequence (5′-PuG*C and 5′-PyG*G).

Et 743 has shown promising activity in phase I and II clinical trials, particularly in soft tissue sarcomas, which sets it apart from other minor groove DNA monoalkylating agents [17,18]. One very unique feature of this agent is that it is the first example of a minor groove alkylating agent that bends DNA toward the major groove [19]. In addition, other factors, such as the sequence-dependent hydrogen-bonding interactions between Et 743 and the minor groove of DNA and the protrusion of the C-subunit from the minor groove, may also contribute to the biological activity of Et 743 [15]. However, the biologically relevant macromolecular targets have not been fully determined. The first proposed target was topoisomerase I, which forms protein–DNA cross-links in the presence of Et 743 [20,21]. More recently, evidence was presented that shows that Et 743 can interfere with transcription activation of the MDR1 gene [22]. The Pommier laboratory has now provided compelling evidence that eukaryotic XPG-defective cells are resistant to Et 743 [23], and the D'Incalci group has shown that XPF–ERCC1-defective cells are also resistant to Et 743 [24]. In this contribution we have tested a panel of eukaryotic cell lines defective in the nucleotide excision repair (NER) pathway for sensitivity to Et 743 and found that they are more resistant than the parent wild-type cell line. To gain further insight into this unexpected result, we have used the bacterial UvrABC nuclease system to characterize how the NER pathway recognizes and repairs Et 743–DNA adducts that differ in their hydrogen-bonding-induced stability in the DNA helix. Significantly, Et 743–DNA adducts at different sequences, with inherently different stabilities, are repaired at different efficiencies. Specifically, the sequences at which Et 743 forms less stable, more dynamically flexible DNA adducts (e.g. at 5′-AGT) are the sites at which repair incision is the most efficient, while the more stable and conformationally rigid Et 743–DNA lesions are not as readily incised. In both cases this can lead to aberrant or uncoupled 3′ or 5′ incisions. This decrease in incision efficiencies at the preferred DNA sequences (e.g. 5′-AGC) compared to the non-preferred sequences (e.g. 5′-AGT) may be explained by defined differences in DNA structure and dynamics induced by binding Et 743 at these different bonding sites. We propose that the inefficient incision repair is related to the repair-dependent toxicities previously

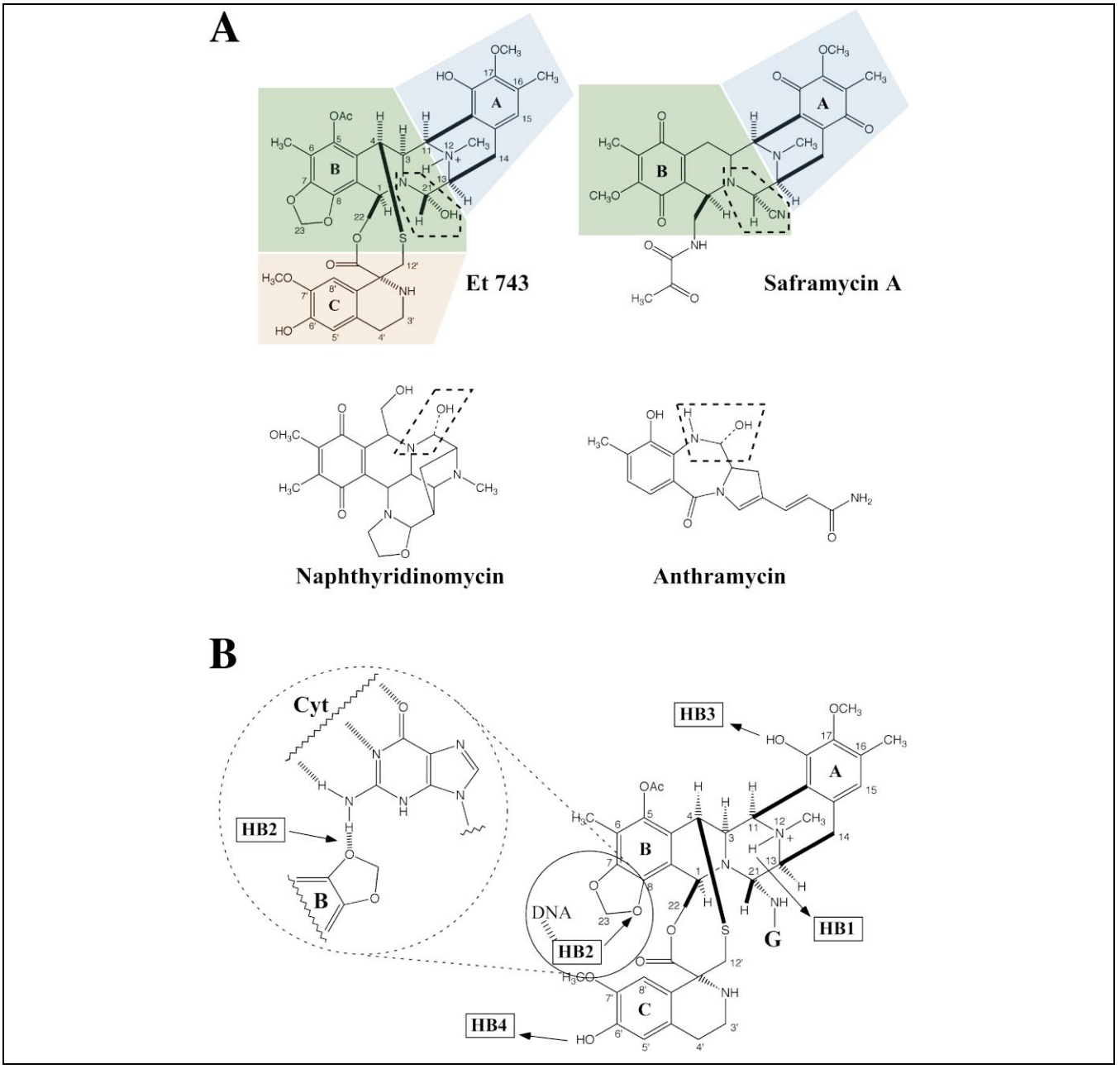

Fig. 1. A: Structures of Et 743, saframycin A, naphthyridinomycin, and anthramycin. Carbinolamines are indicated by a dashed line. A-, B-, and C-subunits of Et 743 and saframycin A are shaded blue, green, and orange, respectively. B: The hydrogen-bonding (HB1–HB4) interaction of Et 743 covalently bound with DNA. HB1–HB3 make direct contacts with the 3-bp DNA target sequence. The direction of arrows refers to hydrogen bond donor to acceptor. In the case of the 5′-AGT sequence, HB2 is lost. The enlarged area shows the HB2 hydrogen-bonding between O18 and the exocyclic 2-amino group of guanine on the 3′-side of the covalent adduct site.

demonstrated in mammalian cells [23,24]. A model is proposed for how the bacterial UvrABC nuclease handles Et 743–DNA adducts at the preferred and non-preferred bonding sequences, which rationalized the NER-dependent toxicity observed in mammalian cells. While the complexity of NER in bacteria and mammalian cells is clearly different, with a larger patch and more proteins involved in the mammalian NER, it is believed that both systems have much in common.

2. Results

2.1. *Mutant cell lines deficient in the transcriptionally coupled NER pathway are more resistant to Et 743 than to their isogenic parent cell line*

Both the Pommier [23] and the D'Incalci [24] laboratories have reported that NER-defective cell lines (XPG– and XPF–ERCC1, respectively) are more resistant to Et

743 than to their isogenic parent cell lines. The results in Fig. 3 demonstrate that all of the mammalian NER-defective cell lines (XPB, XPD, XPF, XPG, and ERCC1) show about a five-fold greater resistance to Et 743 than the Chinese hamster ovary parent cell line (AA8). Of these cell lines, ERCC1 and XPG are more resistant, thus confirming the previous results but extending this observation to all these genes involved in transcriptionally coupled events. Of the other carbinolamine antibiotics shown in Fig. 1B, only anthramycin has been tested for DNA repair. In this case, single- and double-strand breaks were found to be excision repair-dependent [25].

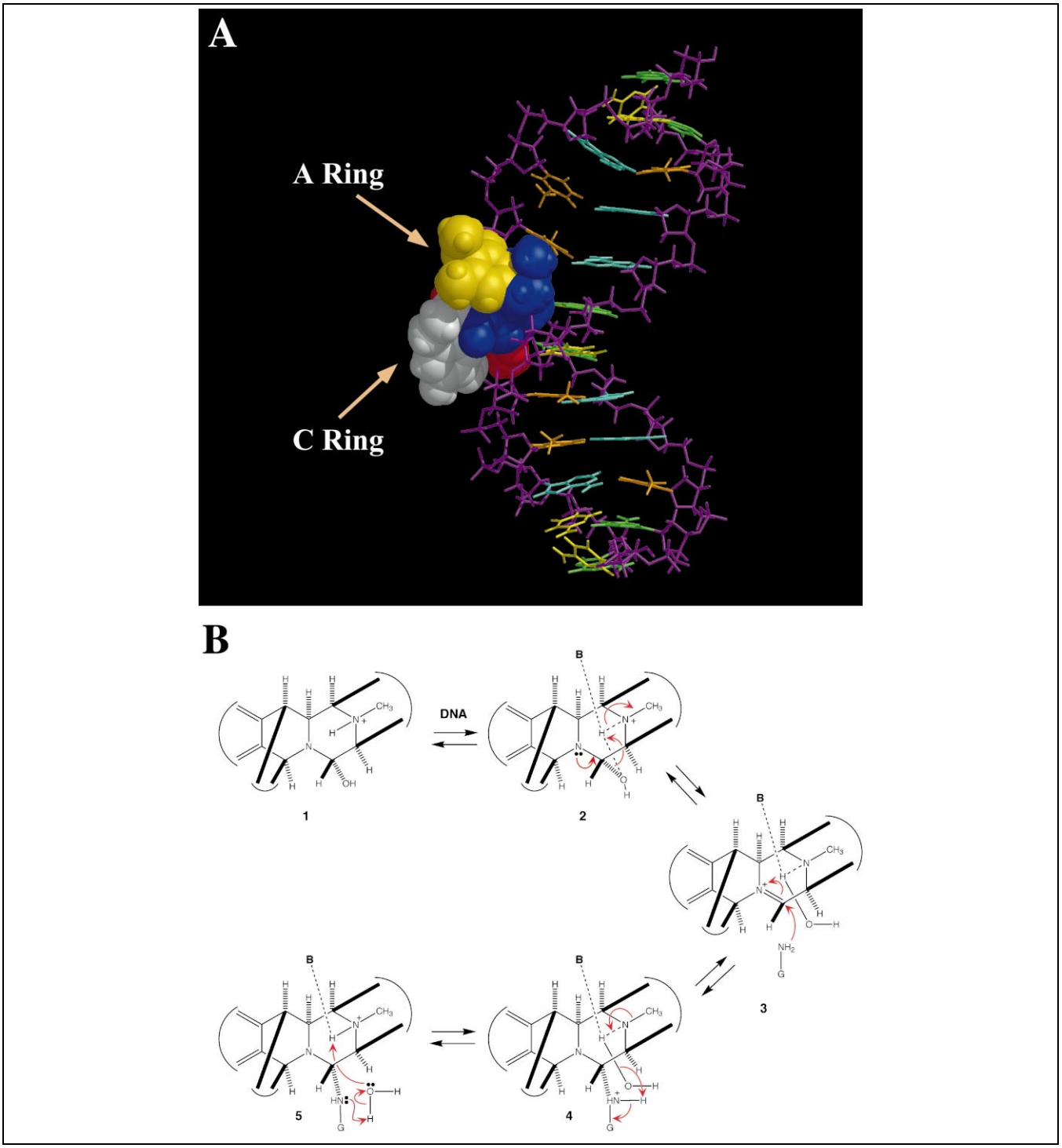

Fig. 2. A: A molecular dynamics-generated structure of Et 743 at the preferred bonding site. The three Et 743 subunits A (green), B (yellow), and C (white) are positioned in the minor groove of DNA. B: Reversible reaction of Et 743 with DNA to form the Et 743–N2-guanine–DNA adduct. 'B' is a DNA base hydrogen bond acceptor (adapted from [16]).

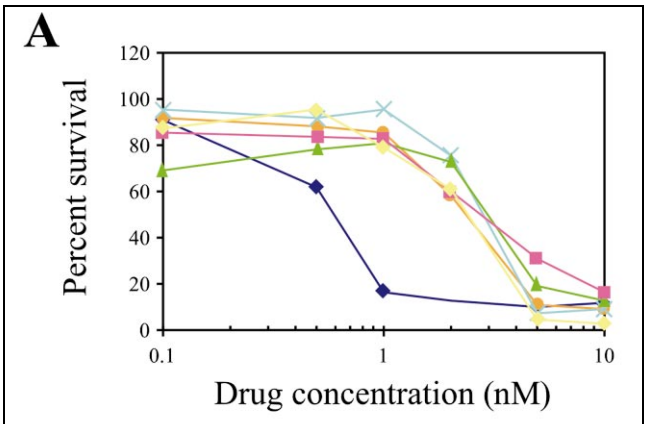

B

Cell lines	IC_{50} values (nM)
AA8 (WT)	0.46
ERCC1 (UV20)	2.22
XPB (UV24)	2.54
XPD (UV5)	2.61
XPF (UV41)	2.88
XPG (UV135)	2.07

Fig. 3. A: Percentage survival of Chinese hamster ovary parent cell line (AA8) and the NER-defective lines (XPB, XPD, XPF, XPG, and ERCC1) in the presence of increasing Et 743 concentrations. B: IC_{50} values for each cell line from (A).

2.2. *Et 743–DNA adducts are recognized and incised by UvrABC nuclease, although at high Et 743 concentrations, the ability of the protein complex to incise these lesions is inhibited*

Since the NER pathway repairs the majority of compounds that covalently modify DNA (for reviews see [26–28] and references therein), and this pathway seems to be detrimental to cellular viability in the presence of Et 743 [23,24], we thought it would be pertinent to determine the ability of the UvrABC nuclease to recognize and incise Et 743–DNA adducts. A restriction enzyme fragment from the adenine phosphoribosyltransferase (APRT) gene modified with various concentrations of Et 743 was incubated with the UvrABC proteins, and the digested substrates were analyzed on a denaturing gel. The UvrABC incision step at the 5′- or 3′-side of the Et 743–DNA adducts can be monitored by radiolabeling the DNA substrate on either the 5′- or 3′-side, respectively. The UvrABC cleavage pattern of the 5′- and 3′-end-labeled DNA fragments from the APRT gene shows that Et 743–DNA adducts are indeed recognized and incised by UvrABC nuclease (Fig. 4A). Notably, the ability of UvrABC nuclease to incise the Et 743–DNA adducts becomes inhibited at the higher Et 743 concentrations (lanes 10 and 11, left and right panels). This phenomenon has been shown with other DNA-interactive compounds such as mitomycin C [29], anthramycin [30], and CC-1065 [31]. One possible explanation for this result is that multiple Et 743–DNA lesions in close proximity distort DNA, thereby preventing the UvrABC nuclease from processing the lesion. A second possibility, which we favor, is that Et 743–DNA adducts could sequester one or more of the UvrABC proteins, rendering them unavailable to efficiently recognize and incise subsequent Et 743–DNA lesions.

2.3. *UvrABC incision frequency of DNA-containing Et 743 adducts is dependent upon sequence context, where adducts at the non-preferred Et 743 target sequences (e.g. 5′-AGT) are incised more efficiently than adducts at the preferred sequences (e.g. 5′-AGC)*

Further analysis of the cleavage patterns of Et 743-modified DNA shows that strand breaks occur three or four bases 3′ to the modified guanine residue and six or seven bases 5′ to the modified guanine residue, which is typical of UvrABC nuclease incision [26,27]. However, quite clearly not all Et 743–DNA adducts are equally incised by UvrABC, as is evident by the varying degrees of the intensities of the strand breaks (Fig. 4A). The relative intensities of each incision product were quantified for both 3′- and 5′-sides of each Et 743–DNA adduct (above and below the sequence in Fig. 4B). Intriguingly, the Et 743–DNA adducts at the non-preferred sequences (i.e. 5′-AGT and 5′-TGT) are incised with the highest efficiency, whereas adducts at the preferred sequences (5′-AGC and 5′-TGC) were incised to a lesser extent (compare incision bands 19 and 30 with bands 11 and 16 in Fig. 4B).

To increase the data set and confirm that Et 743–DNA adducts at the non-preferred sequences are truly incised more efficiently than at the preferred sequences, we examined two other DNA restriction enzyme fragments: a 209-bp fragment from the pCAT plasmid and a 200-bp segment from the pBR322 vector. Consistent with the previous results (shown in Fig. 4A,B), both of the new Et 743-modified restriction enzyme fragments showed inhibition of incision at high Et 743 concentrations and displayed differential incision that was dependent upon the immediate DNA flanking sequence (data not shown). The intensities of the bands corresponding to the 3′ and 5′ incision sites were scanned, and the relative intensities of each band are shown above and below the sequences in Fig. 4C,D, for each of the two DNA fragments. For the most part, the guanines that render a strong 5′ incision band also render a strong 3′ incision band. Again, the most striking result is that the highest UvrABC incision efficiencies occur for the non-preferred DNA sequences that form the unstable DNA adducts in both the pCAT and pBR322 DNA fragments.

The data for all the UvrABC incision results have been pooled and accumulated in Fig. 5. For the preferred and non-preferred sequences (Fig. 5A,B), the efficiency of each 3′ and 5′ incision was categorized into high, moderate, or low. It is clear from a comparison of panels A and B in

Fig. 5 that the Et 743–DNA adducts at non-preferred sequences that lack the ability to form the HB2 hydrogen bond (see Fig. 1B) are incised at a higher efficiency than those that can form the complete hydrogen bond network. Adducts at the preferred alkylation sites that form the HB2 hydrogen bond are incised with moderate to low efficiency (Fig. 5A), while adducts at the non-preferred sequences display incision frequencies that are more even, cutting at high, moderate, or low efficiencies (Fig. 5B). In addition, about 25% of the preferred target sequences show no incision 5′ or 3′ to the Et 743–DNA adduct, whereas all the non-preferred sites showed at least 3′ or 5′ incision. It is important to recognize that the actual percentage of the Et 743 adducts that are incised by UvrABC are not adjusted for the extent of modification of guanines to a given site. It is likely that the actual percentage of Et 743-induced modification at the preferred sequences is even higher than that at the non-preferred target site, since the DNA adducts at these sites are more stable at these sequences [16]. Thus, the actual extent of difference between incision frequency at preferred and non-preferred sequences is likely to be underrepresented. There is an apparent low frequency of uncoupled 3′ or 5′ incisions for both preferred and non-preferred sequences (usually less than 10%). We are hesitant to make too much of the significance of this result because of its minor contribution and because the absolute assignment of the 3′ or 5′ incisions can be sometimes confused by the aberrant 5′ cleavage bands observed in the site-directed Et 743–DNA adducts.

2.4. *The flanking sequence outside the 3-bp target sequence (5′-NGN) may contribute to the efficiency of incision of Et 743–DNA adducts by UvrABC nuclease*

Further inspection of the data in Figs. 5 and 6 demonstrates that not all of the Et 743–DNA adducts at the same 3-bp target sequence are incised at the same efficiency, suggesting that more than just the 3-bp recognition sequence is involved in determining the efficiency of incision by the UvrABC nuclease. For example, the highest level of incision occurs for a 5′-TGT lesion (site 30 in Fig. 4B) in the DNA fragment from the APRT gene, but Et 743–DNA adducts at other 5′-TGT sequences surrounded by a different flanking sequence show different levels of incision (compare incision sites 1, 2, 15, and 30 in Fig. 4B). In another example, a 5′-AGT adduct site placed next to an A-tract was not incised efficiently (compare

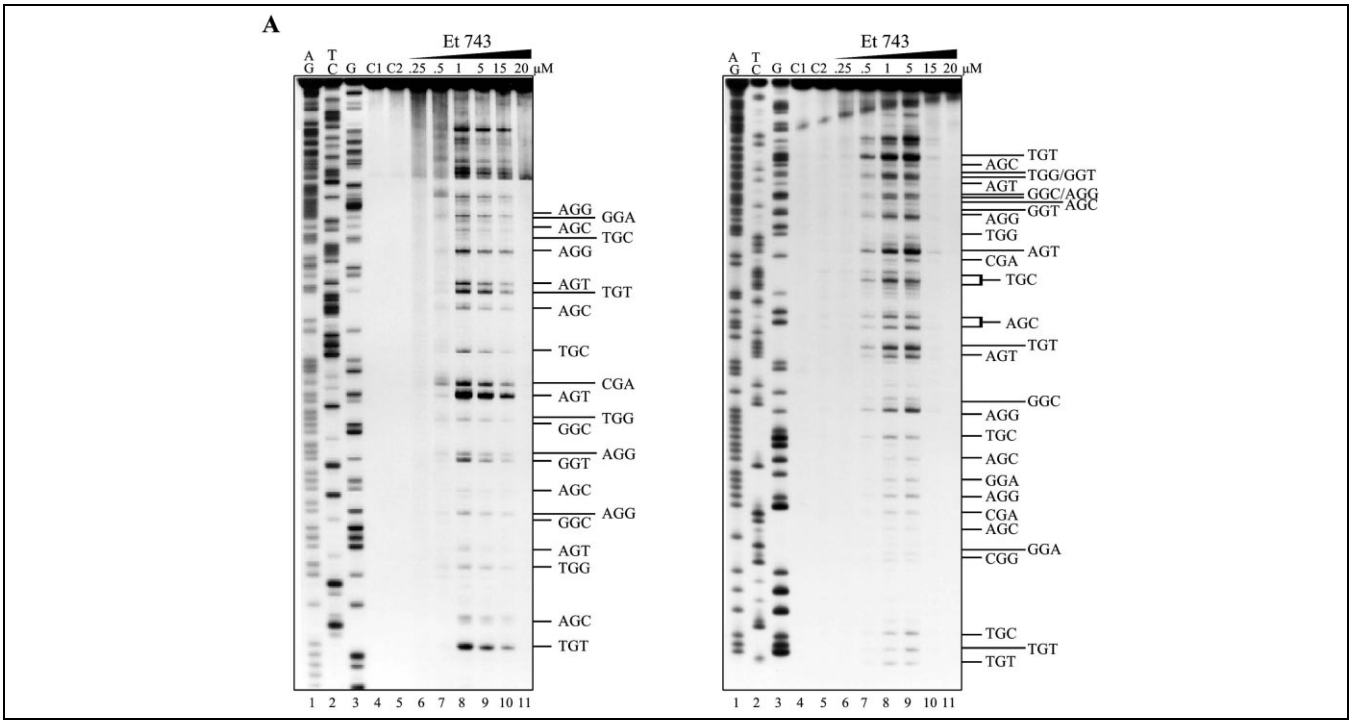

Fig. 4. A: Autoradiogram of UvrABC nuclease incision of an Et 743-modified 5′- or 3′-end-labeled 188-bp DNA fragment from the Chinese hamster ovary APRT gene. Lanes 1–3, Maxam–Gilbert chemical sequencing reactions; lane 4 (control), DNA treated with 5 μM of Et 743; lane 5, unmodified DNA treated with UvrABC; lanes 6–11, DNA modified with 0.25, 0.5, 1, 5, 15, and 20 μM of Et 743, respectively, in the presence of UvrABC. The Et 743 target sequence corresponding to the drug modification-induced UvrABC nuclease incision bands is shown on the right side of each panel. B: Relative intensities of UvrABC nuclease incision on the 3′- and 5′-sides of Et 743–DNA adducts in the 188-bp sequence from the APRT gene. The intensities were normalized to 100% for the most intense band in each experiment. Arrows highlight some of the Et 743-modified AGC and AGT sequences that are incised to varying degrees. C and D: Relative intensities of UvrABC nuclease incision on the 3′- and 5′-sides of Et 743–DNA adducts in the 209-bp fragment from pCAT plasmid (C) and the 200-bp fragment from pBR322 vector (D). The intensities were normalized to 100% for the most intense band in each experiment. (●) indicates guanines that show no incision on either the 5′- or 3′-side of the Et 743–DNA adducts.

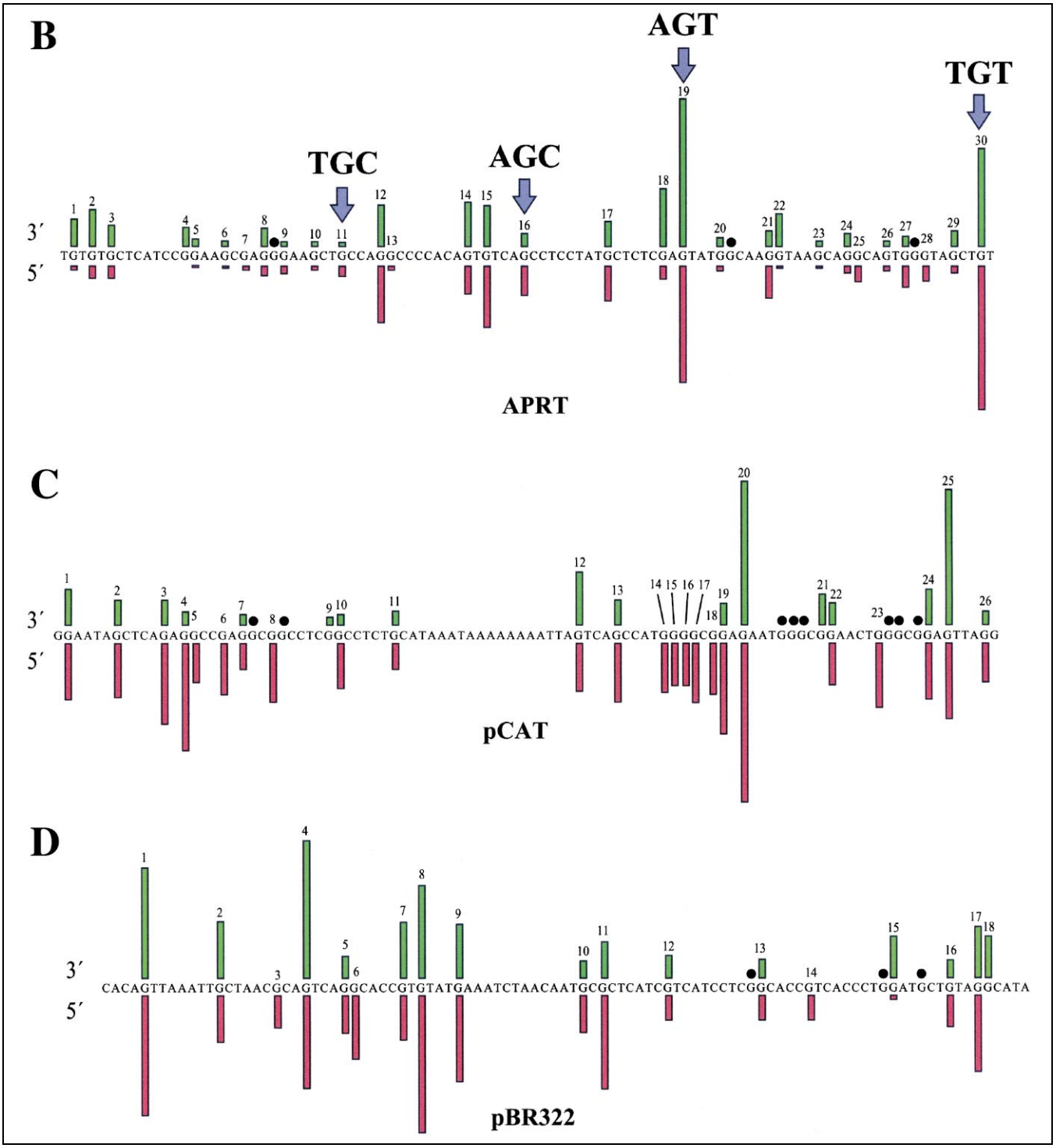

Fig. 4 (*continued*).

incision sites 12 and 25 in Fig. 4C). While no obvious consensus sequence could be inferred for identical Et 743 bonding sites that were efficiently incised versus the adduct sites that were poorly incised, we have shown previously that certain sequences, such as an A-tract, can contribute to the overall stability of Et 743–DNA adducts [16]. Therefore, it is not too surprising that the flanking region beyond the 3-bp Et 743 recognition sequence also plays an important role in determining the UvrABC efficiency of the incision process.

2.5. *UvrABC nuclease displays anomalous DNA incision of Et 743–DNA adducts showing an extra incision product 11 or 13 bases 5′ to the lesion*

An Et 743-modified 64-bp fragment (see Fig. 6A,B) was

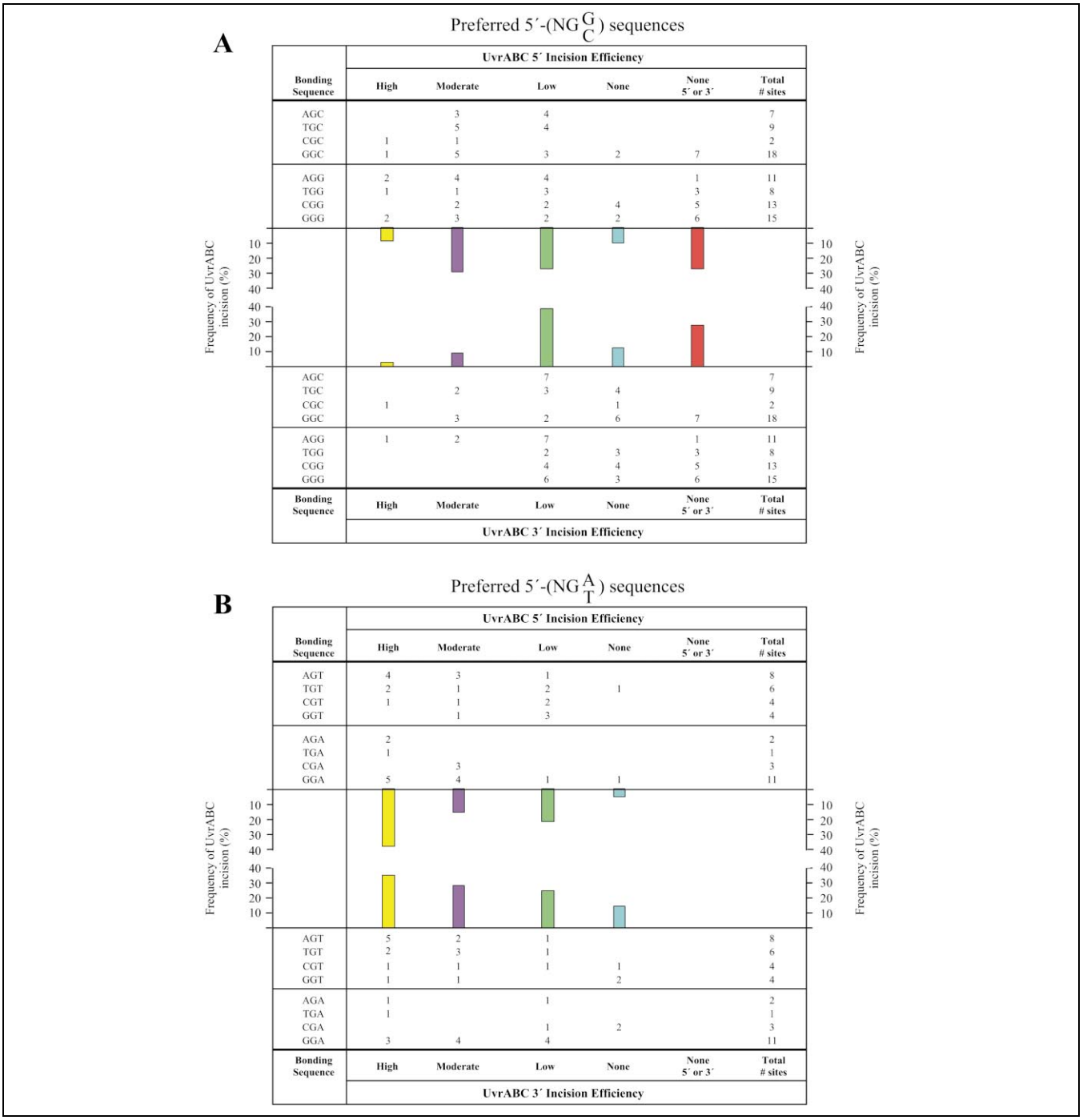

Fig. 5. A and B: Summaries of the UvrABC nuclease incisions on the 5′- and 3′-sides of the Et 743–DNA adducts at the 5′-(NG$^{G}_{C}$) and 5′-(NG$^{A}_{T}$) 3-bp recognition sequence. Numbers refer to the number of times the Et 743–DNA adduct was incised high, moderate, or low for a given recognition sequence. Each bar (expressed as a percentage) represents the number of times the non-preferred or preferred binding sites were incised high, moderate, or low by UvrABC. The intensity of each band was normalized to the highest intensity band (100%). 1–20% is defined as low, 21–44% is moderate, and 45–100% is high.

used to study the UvrABC incision of a DNA duplex containing either a centrally located 5′-AGC or 5′-AGT sequence. Both 3′- and 5′-end-labeled fragments were used on the (+) and (−) strands in these experiments. This Et 743 alkylation site is located within a central 22-bp segment that is made up entirely of AT base pairs. Due to the self-complementarity of the region containing the 5′-AGC sequence (Fig. 6A), there is an Et 743-reactive guanine in the 5′-AGC sequence located on both the top and bottom strands. As a result, Et 743 can modify either strand. Both duplexes were modified with Et 743 followed by incubation with the UvrABC proteins, and the results are shown in Fig. 6A,B.

Surprisingly, the UvrABC incision 5′ to the Et 743–

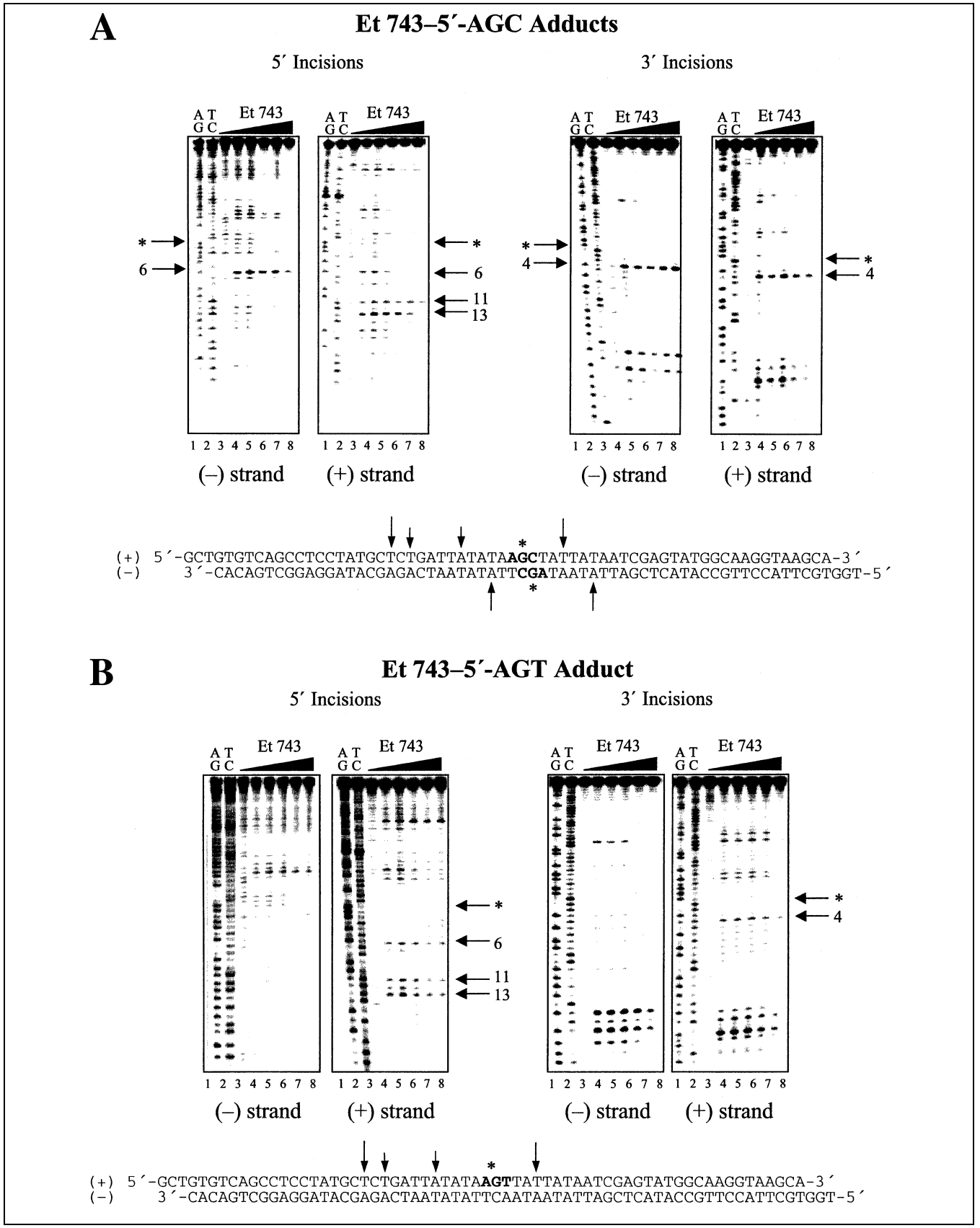

Fig. 6. Autoradiogram showing the 5′ and 3′ incisions of the 64-bp DNA oligonucleotide containing the (A) 5′-AGC or (B) 5′-AGT sequence. DNA was modified with 0, 0.5, 1, 2.5, 5, or 10 μM (lanes 3–8) of Et 743 followed by incubation with UvrABC. Arrows denote the sites of UvrABC incision. (*) indicates the 5′-AGC and 5′-AGT alkylation sites of Et 743. AG and TC refer to the Maxam–Gilbert sequencing lanes. The other sites of incision arise from other Et 743–DNA alkylation sites. The full 64-bp sequence, with the bonding site highlighted and incision sites shown by arrows, whose lengths correspond to intensity of cleavage, is shown at the bottom of each panel.

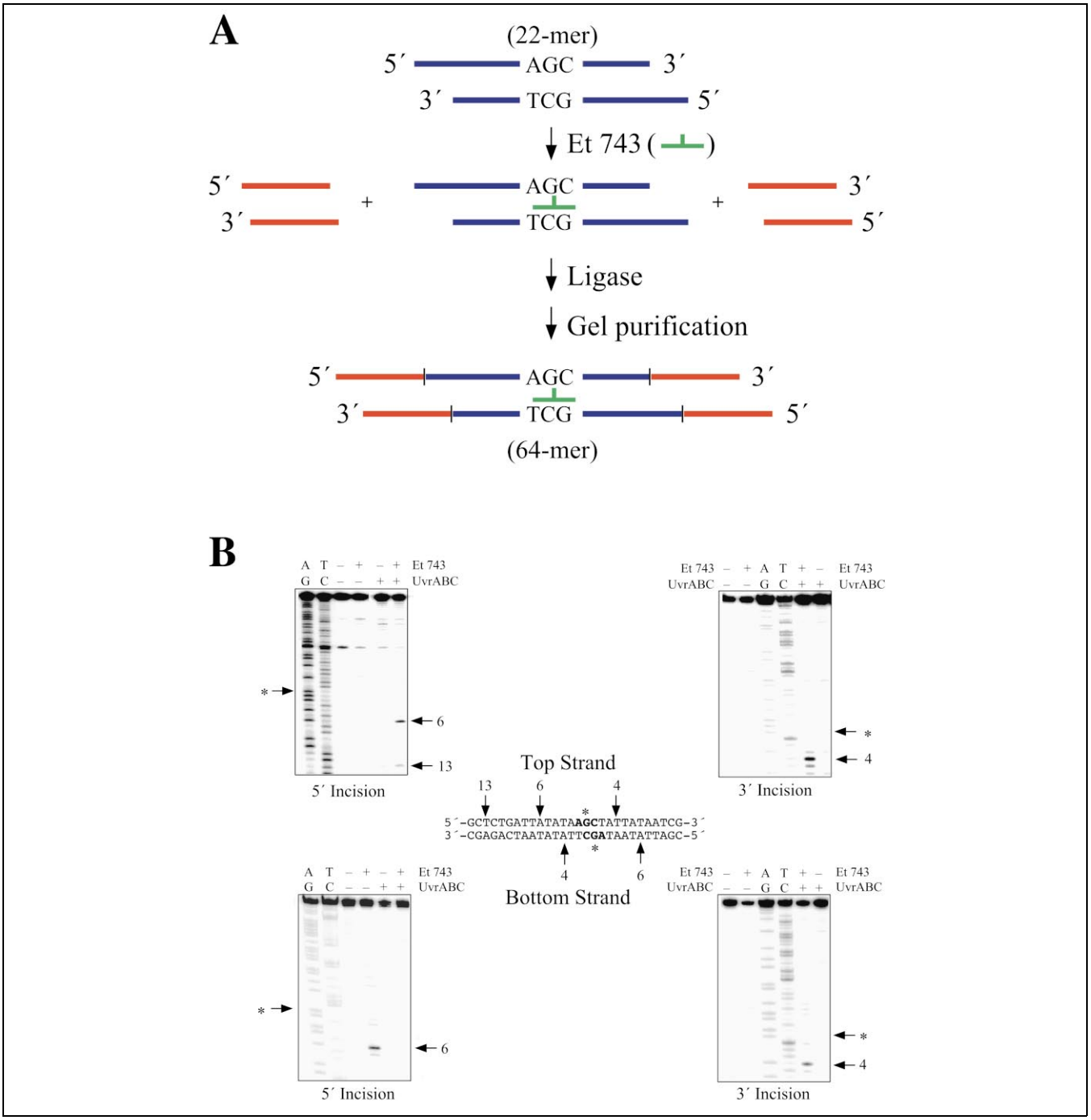

Fig. 7. A: Schematic for the preparation of the Et 743 site-directed adduct. B: Reaction of the UvrABC nuclease with either a top or bottom strand 5′- or 3′-end-labeled DNA sequence containing an Et 743–DNA site-directed adduct. Modification of DNA by Et 743 was as shown for Fig. 6. The UvrABC incision sites are indicated by arrows. AG and TC refer to Maxam–Gilbert sequencing lanes. (*) indicates the 5′-AGC alkylation site. The central sequence shows the incision pattern for UvrABC nuclease.

DNA adduct is not the same for both strands. As expected, the 5′ incisions for the top and bottom strands occurred six bases from the adduct; however, 5′ incisions also occurred 11 and 13 bp from the adduct on the top strand (Fig. 6A, left panel). The 3′ incision occurred four bases away from the site of the Et 743–DNA lesion for both strands (Fig. 6A, right panel). That the intensity of the 3′ strand incisions is nearly equivalent for the products on the top and bottom strands of the 5′-AGC adduct argues that Et 743 alkylates both strands equally. The extra incisions on the 5′-side also occurred for the sequence containing the 5′-AGT adduct on the top strand (Fig. 6B, left panel), indicating that, in this case, the anomalous incision is independent of the 3-bp Et 743 target sequence. It is surprising that the extra incisions occur only on the top strand. The explanation must be that

although the 5′-AGC sequences on the top and bottom strands are both contained within an A/T-rich region, the flanking sequences are not identical. Presumably UvrABC is able to recognize differential structural or dynamic features between Et 743–DNA adducts on the top and bottom strands. Extra 5′ incisions have also been reported for cisplatin [32], where two major incision products occurred 8 and 15 bases from the site of the lesion. However, a more defined system seemed necessary since the sequences shown in Fig. 6A,B contained other Et 743 alkylation sites in flanking regions, which when alkylated could potentially interfere with UvrABC incision at the 5′-AGC and 5′-AGT adduct sites. Hence, we created a site-directed Et 743–DNA adduct with the same sequence as that used above.

2.6. UvrABC incision of a DNA fragment containing a site-directed Et 743–DNA adduct in the preferred 5′-AGC sequence shows anomalous cleavage

In all the previous experiments, there was potential for overlap of UvrABC repair incision sites due to multiple Et 743–DNA adducts, and consequently the results were sometimes difficult to interpret unambiguously. In a subsequent experiment, we attempted to create a more defined system. Specifically, we carried out parallel UvrABC nuclease experiments on Et 743–DNA site-directed adducts containing either the preferred 5′-AGC sequence or the non-preferred 5′-AGT sequence. Since Et 743 reacts only with duplex DNA and not single-stranded DNA, the preparation and purification of Et 743–DNA adducts were restricted to duplex DNA substrates. The strategy used for the preparation of 5′-AGC, the site-directed adduct, is shown in Fig. 7A. The Et 743–DNA site-directed adduct was created by ligating a 22-bp Et 743-modified duplex containing either a single 5′-AGC or 5′-AGT sequence to a pair of double-stranded DNA oligonucleotides, using different sticky ends to unambiguously ligate one on each side of the Et 743-modified duplex. This resulted in the construction of a 64-bp fragment containing the same sequence used in the prior section. While the creation of an Et 743 site-directed adduct containing the preferred 5′-AGC sequence was successful, repeated attempts to generate the Et 743–5′-AGT DNA adduct failed. This is presumably because the Et 743–DNA adduct at the 5′-AGT sequence underwent covalent reversal during purification due to its intrinsic instability [16]. Therefore, only the 64-bp site-directed Et 743–DNA adduct containing the 5′-AGC target sequence was used to study the pattern of incision by UvrABC.

Fig. 7B shows the results of four experiments using both strands having either the 3′- or 5′-radiolabeled site-directed 5′-AGC adduct after incubation with the UvrABC nuclease. 5′ incision occurs both 6 and 13 bases from the covalent attachment site on the top strand, whereas on the bottom strand 5′ incision only occurs six bases from the Et 743 adduct site. The 3′ incision events occur equally well on both strands and show only one incision product four bases from the Et 743-damaged guanine. The results presented here substantiate our previous results (shown in Fig. 6A), in which anomalous incision occurs only on the top strand on the 5′-side, while the incision occurs on the bottom strand at the expected sites, i.e. six bases 5′ and four bases 3′ to the Et 743-alkylated guanine, for a DNA duplex containing a 5′-AGC sequence.

3. Discussion

Et 743 is a structurally and mechanistically unique antitumor antibiotic that has shown very encouraging antitumor activity in phase I and II clinical trials, particularly in soft tissue sarcomas. Because of the implications of the involvement of NER in mediating the biological potency, and perhaps specificity, of this compound (see Fig. 3), we set out to study the recognition and incision of Et 743–DNA adducts using the *Escherichia coli* UvrABC nuclease. While the human NER system is more complex, involving a larger number of repair proteins, and the repair patch is larger than in the bacterial system, the basic mechanism is similar in both systems. In the UvrABC system, repair is initiated by the UvrA protein, which dimerizes prior to formation of a heterotrimeric complex with UvrB [33,34]. This $UvrA_2B$ complex has helicase-like properties and specifically binds to damaged DNA [35,36]. Binding of the $UvrA_2B$ complex to duplex DNA results in both bending of the DNA and an open DNA structure [35,37,38]. After damage recognition, UvrA dissociates, while UvrB remains bound to the damaged DNA in a stable preincision complex [39,40]. Following the binding of UvrC to this complex, incision is triggered on both sides of the damaged site: four nucleotides 3′ to the damaged site and seven nucleotides 5′ to the same site [37,41–43]. The repair is completed by UvrD, DNA polymerase, and DNA ligase. Much remains to be learned about the structural biology of the discrimination between non-damaged and damaged DNA and the structures of the various complexes of $UvrA_2$, $UvrA_2B$–DNA, UvrB–DNA, and UvrBC–DNA. A crystal structure of UvrB has recently been published and a model of the UvrB–DNA complex has been proposed [36]. We propose a model for how Et 743–DNA adducts are processed by bacterial and human cells to result in the repair-dependent toxicity to cells. This model takes into account both the unique structural and dynamic features of the Et 743–DNA adducts and the resistance of mammalian cells to the toxic effects of Et 743, which are defective in NER repair proteins involved in assembly of a repair complex competent to perform 3′ and 5′ incision steps.

3.1. The efficiency of UvrABC incision of Et 743–DNA adducts is dependent upon the stability of the bound adduct at the target sequence, and in some cases, the 3′ and 5′ incisions are absent or they occur at aberrant sites

There is a clear difference in the efficiency of the UvrABC incision of Et 743–DNA adducts that is dependent upon the precise Et 743 bonding sequence. The results summarized in Fig. 5A,B show that Et 743–DNA adducts bound to 5′-AGT sequences are much more efficiently incised by UvrABC nuclease than the same adducts bound to 5′-AGC sequences. In a previous study [16] we demonstrated that the presence or absence of specific hydrogen-bonding interactions between donors and acceptors on Et 743 and the 3-bp recognition sequence leads to significant differences in the stability and conformational flexibility of the resulting DNA adducts. Of prime importance is the presence or absence of a hydrogen-bonding interaction between O18 of the methylenedioxy ring and the exocyclic 2-amino group of guanine on the 3′-side of the alkylated guanine, which may be on either the covalent or non-covalently modified strand (see Fig. 1B). Of less significance are the hydrogen-bonding interactions on the 5′-side of the covalently modified guanine. In the absence of a 3′ GC base pair, which provides this crucial hydrogen-bonding, Et 743–DNA adducts more easily undergo covalent reversal and show weaker base-pairing forms and alternative base-pairing conformers on the 5′-side [16]. Furthermore, as anticipated, helicase-catalyzed unwinding of DNA using T-antigen or thermal denaturation results in enhanced instability of the Et 743–5′-AGT duplex adducts over the corresponding 5′-AGC duplex adducts [16]. Therefore, there is an inverse correlation between Et 743–

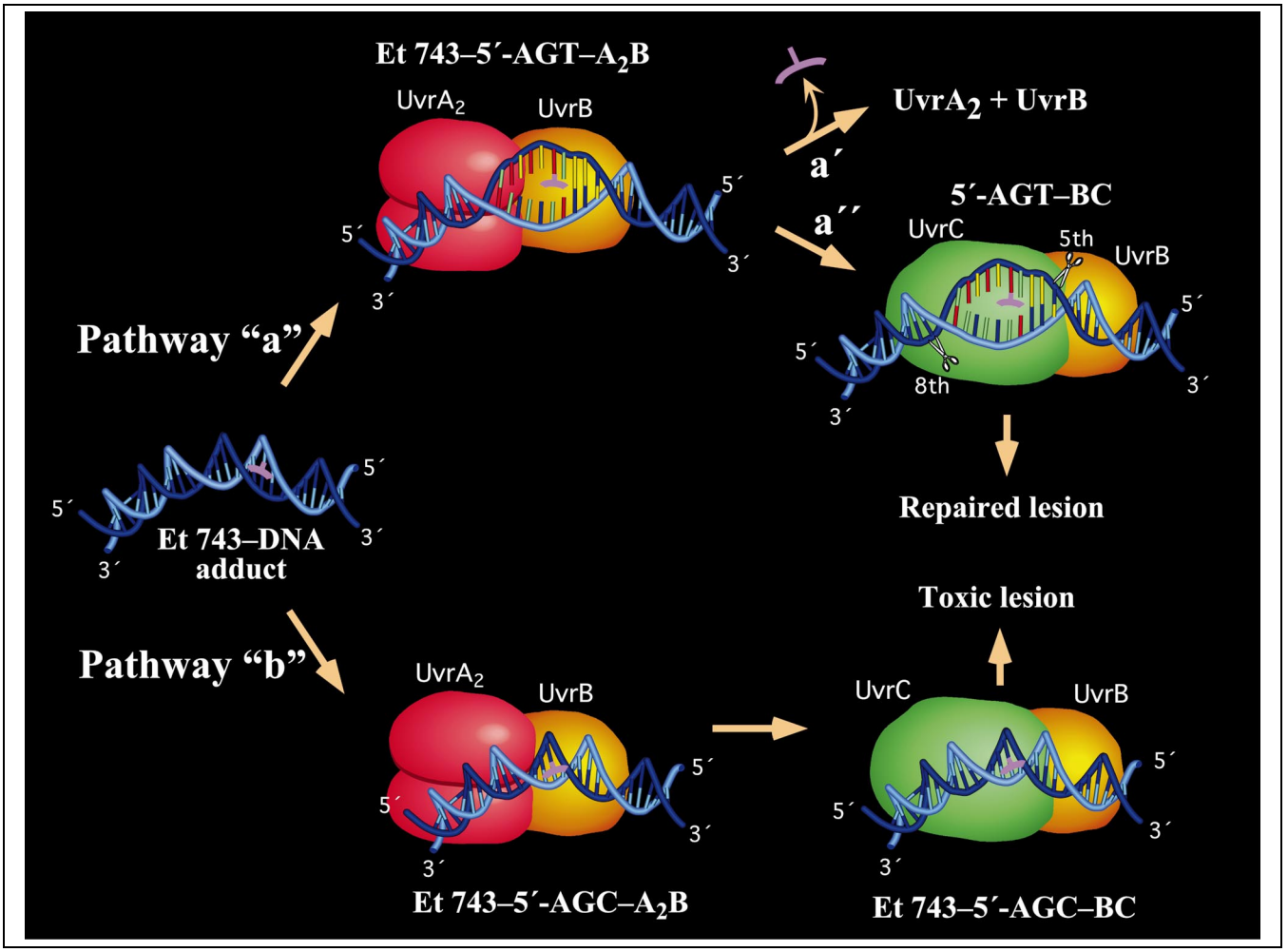

Fig. 8. Proposed model for how UvrABC nuclease may process Et 743–DNA adducts, leading to either a repaired lesion (pathway ‘a’) or a toxic lesion (pathway ‘b’) corresponding to the mammalian NER-dependent toxicity. In pathway ‘a’, $UvrA_2B$ is able to recognize the Et 743 and unwind the duplex DNA, creating the bubble that positions the Et 743–DNA adduct in a region of single-strandness, which leads to covalent reversal of the Et 743–DNA adduct (a′) or to 3′ and 5′ incisions (a″). For pathway ‘b’, an optimally stabilized Et 743–DNA adduct is in a region of bent DNA, which is recognized and bound by the $UvrA_2B$ complex. In this case the Et 743–DNA duplex adduct mimics the normally unwound form of modified DNA bound to $UvrA_2B$, A_2 dissociates, and then C binds to form the Et 743–BC complex. This substrate is inefficiently incised by UvrBC, which results in the absence of 3′ and 5′ incisions. This leads to the toxic lesion mechanistically equivalent to a drug-poisoned topoisomerase I– or topoisomerase II–DNA complex.

DNA adduct stability and UvrABC incision efficiency. This point is further exemplified by a comparison of the UvrABC incision efficiency of Et 743–5′-AGT adducts in different sequence contexts. Et 743–5′-AGT adducts adjacent to A-tracts are much less efficiently incised than the same adducts without flanking A-tracts. In a previous study [16] we demonstrated that A-tracts stabilize Et 743–DNA adducts to covalent reversal, which we have attributed to dampening the conformational flexibility of Et 743–5′-AGT adducts and strengthening the apparent hydrogen-bonding interactions.

Irrespective of the covalent bonding sequence, Et 743–DNA adducts appeared to show some uncoupled 3′ and 5′ incisions (Fig. 5A,B), although the combination of the low frequency of these events and their sometimes ambiguous assignment makes this conclusion less than firm. The absence of both 3′ and 5′ incisions is found only for the 5′-AGC Et 743 bonding sequences. Thus it would appear that for loss of both 3′ and 5′ incisions, the hydrogen-bonding donor/acceptor pair between Et 743 and the GC base pair immediately to the 3′-side of the Et 743–DNA adduct is required. Last, aberrant UvrABC incisions occurring 11 or 13 bases to the 5′-side of the Et 743–DNA adducts are found for both 5′-AGT and 5′-AGC bonding sites.

3.2. Inefficient 3′ and 5′ incisions by NER complexes lead to cytotoxic effects of Et 743–DNA adducts in human cells

In contrast to the *E. coli* UvrABC nuclease, where the UvrC and UvrB proteins give rise to the 5′ and 3′ incisions, in human NER the dual incisions at the 5′- and 3′-sides of the DNA adducts are carried out by two physically separated nuclease activities: XPG– and XPF–ERCC1, respectively. Human cells lacking either of these nucleases are resistant to Et 743 [23,24]. Furthermore, the results in Fig. 3 show that other defective proteins involved in the formation of the NER nuclease complex also show resistance to Et 743. Therefore, any model of how Et 743 exerts its cytotoxic potency via the NER pathway must take into account how this NER nuclease complex might result in structural consequences that are detrimental to cell survival.

3.3. In addition to a sequence-dependent hydrogen-bonding stabilization of the Et 743–DNA adduct, Et 743–DNA adducts have other unique structural effects on DNA

NMR studies on covalent oligomer duplex adducts of Et 743 and non-denaturing PAGE analysis of ligated oligomers containing defined Et 743–DNA adducts reveal important novel characteristics of Et 743–DNA adducts. While Et 743 modifies duplex DNA within the minor groove (Fig. 2A), it also bends DNA into the major groove [19]. This results from the wedge shape of Et 743, which forces open the minor groove of DNA and concomitantly closes up the major groove. In addition to the major groove bending and minor groove occupancy, the C-subunit of Et 743 protrudes outside the helical axis occupied by duplex DNA (Fig. 2A). In summary, the covalent attachment of Et 743 to DNA and flanking donor/acceptor hydrogen-bonding of DNA zipper up a locally widened minor groove of DNA, which also has an extrahelical protrusion in an otherwise bent DNA. Somehow these unique structural characteristics of Et 743–DNA adducts must result in the reduced efficiencies of the sequence-dependent UvrABC nuclease incision and the uncoupled or absent 3′ and 5′ UvrABC incisions observed in this study, along with the NER-dependent cytotoxicities observed in human cells. In Section 3.4 we propose a model that takes into account all of these observations with what is known about NER in *E. coli* and human cells.

3.4. Model for how the inhibited repair of Et 743–DNA adducts can lead to NER-mediated cytotoxicity

As previously described, $UvrA_2B$ complex detection of damaged DNA is proposed to lead to a 6-bp bubble around the modified based and to bending of the DNA [35]. This then results in dissociation of $UvrA_2$ from the complex, leaving a UvrB–DNA complex that is a stable preincision complex. UvrC is then recruited, which results in endonuclease cleavage by UvrC 3′ and 5′ to the adduct site [44] (see pathways ‘a’ and ‘a‴’ in Fig. 8). Dependent upon the stability of the Et 743–N2-guanine DNA adduct in the 6-bp bubble, the Et 743–N2-guanine covalent linkage may reverse before the 3′ and 5′ incisions occur (pathways ‘a’ and ‘a′’ in Fig. 8). These pathways are most likely in the unfavored sequences for Et 743–DNA adduct stability, where bubble formation is most likely, due to the lack of the additional H-bonding 5′ to the covalently modified guanine (see Fig. 1B). Neither pathway ‘a’ scenario would be predicted to give rise to the repair-dependent enhanced toxicities observed in mammalian cells.

However, processing of Et 743–DNA lesions by pathway ‘b’ (Fig. 8) is predicted to give rise to a toxic lesion. We propose that the unique properties of specific Et 743–DNA adducts lead to malfunction of the UvrABC nuclease system, leading to inefficient incisions on both the 3′- and 5′-sides and, in some cases, possibly uncoupled 3′ and 5′ incisions. Why does an encounter between the UvrABC nuclease system and the hydrogen-bonded stabilized Et 743–DNA adduct lead to aberrant DNA repair?

First, Et 743–DNA adducts may be particularly difficult to process because of their resistance to the helicase activity of the $UvrA_2B$ complex, primarily arising from the zipper-like effects of the hydrogen-bonding stabilization on both sides of the covalent adduct. This is analogous to resistance of stable Et 743–DNA adducts to T-antigen unwinding [16].

It is most likely to be those Et 743–DNA adducts that are resistant to the helicase activity of $UvrA_2B$ that lead to the excision-dependent cytotoxicity (i.e. Et 743–DNA adducts at preferred sequences). In order for incision to occur, UvrA must dissociate and the stable preincision complex of UvrB must be recognized by UvrC to form the active UvrBC nuclease (pathway 'b' in Fig. 8).

Second, we propose that the stable Et 743–DNA duplex adducts must have structural features that somehow mimic the bent and open form of the normal $UvrA_2B$ heterotrimeric complex with DNA. Indeed, Et 743–DNA adducts are bent into the major groove through minor groove expansion due to occupancy by the wedge-shaped Et 743. The extrahelical protrusion of the C-subunit of Et 743 may also play a role in promoting the dissociation of UvrA and, perhaps, stabilizing the UvrB preincision complex. However, in the absence of defined structural interactions among the various protein–DNA components of the $UvrA_2B$–, UvrB–, and UvrBC–DNA complexes, it is impossible to be more specific than just suggesting possible structural mimics (bending) and steric interactions (extrahelical protrusion) that could lead to aberrant DNA repair outcomes. One could envisage a situation similar to that of a drug-poisoned topoisomerase I or II complex where a drug molecule intercepts an intermediate in which neither a 3′ nor a 5′ incision is made but the UvrBC, or even the UvrABC, is trapped as a non-covalent protein–Et 743–DNA complex, which is more detrimental to cells than the original Et 743–DNA adduct. Just as with the drug-poisoned topoisomerase I or II complexes, where elevated levels of topoisomerases would lead to populations of more susceptible cells, a similar situation exists for elevated levels of NER proteins. Some of these possibilities are being explored.

4. Significance

The pattern of inefficient repair incision by the UvrABC nuclease of Et 743–DNA adducts provides a basis for rationalizing the observed repair-dependent cytotoxicities of these DNA adducts, if other associated structural properties of Et 743–DNA adducts are taken into account. On the basis of promising activity in phase I clinical trials, Et 743 has progressed into phase II clinical trials, where it has shown remarkable activity in soft tissue sarcomas. This is the first of the monoalkylating minor groove-interactive agents to progress beyond phase I clinical trials. In previous studies we have determined the structure of the Et 743–DNA covalent adduct, its effect on DNA structure, and the hydrogen-bonding interactions, which determine DNA sequence selectivity and enhanced stability on DNA. These properties set Et 743 apart from other minor groove alkylating compounds. Recent results from groups in Italy (D'Incalci lab) and at NCI (Pommier lab) provide insight into the molecular targets for Et 743, which appear to be proteins involved in the NER pathway. We have confirmed this conclusion, but what is most significant is that we have identified what is likely to be the structural and biochemical basis for the NER-dependent cytotoxicity of the Et 743–DNA adducts. These results link the structural biology of the Et 743–DNA adducts with the biological consequences of incomplete DNA repair. This result is somewhat reminiscent of the formation of cleavable complexes with topoisomerase I– and topoisomerase II–DNA adducts.

5. Materials and methods

5.1. Materials

Ecteinascidin was generously supplied by PharmaMar, Madrid, Spain.

5.2. Cell lines and culture conditions

The Chinese hamster ovary parent cell line (AA8) and the NER-defective cell lines XPB, XPD, XPF, XPG, and ERCC1 were purchased from American Type Culture Collection. All cell lines were grown as a monolayer in Dulbecco's modified Eagle's medium (Gibco, #10-013-CV) supplemented with 1% (v/v) penicillin (100 U/ml), streptomycin (100 μg/ml), and 10% fetal bovine serum. Cells were grown at 37°C in a 5% CO_2 humidified incubator. Trypsin–EDTA solution was used for detaching cells.

5.3. Cytotoxicity assay

A colorimetric assay based on the ability of viable cells to reduce the tetrazolium salt MTS (CellTiter 96 Non-Radioactive Cell Proliferation Assay, Promega Corp., Madison, WI, USA) to a blue formazan product was used to measure cytotoxicity following exposure to Et 743. Cells were plated in a 0.1 ml medium on day 0 in 96-well microtiter plates (Falcon, #3072). On day 1, 10 μl of serial dilutions of the test agent was added in replicates of four to the plates. After incubation for 4 days at 37°C in a humidified incubator, 2 μl of a 20:1 mixture of 3-(4,5-dimethylthiazol-2-yl)-5-(3-carboxymethoxyphenyl)-2-(4-sulfophenyl)-2*H*-tetrazolium, inner salt MTS (2 mg/ml) and an electron coupling reagent, phenazine methosulfate (0.92 mg/ml in DPBS), was added to each well and incubated for 4 h at 37°C. Absorbance was measured using a Model 7520 microplate reader (Cambridge Technology, Inc.) at 490 nm. Data were expressed as the percentage of survival of control calculated from the absorbance corrected for background absorbance. The surviving fraction of cells was determined by dividing the mean absorbance values of the test agents by the mean absorbance values of untreated control.

5.4. Et 743–DNA bonding

Specific amounts of drug were added to radiolabeled DNA in 10 mM Tris–HCl (pH 7.5) and 25 mM NaCl buffer to give the desired final concentration. The solutions were incubated at room temperature for either 1 or 2 h. The unreacted drug was removed by phenol–chloroform extraction.

5.5. Purification of UvrABC proteins

UvrA, UvrB, and UvrC proteins were isolated from *E. coli* K12 strain CH292 carrying plasmids pUNC45 (UvrA), pUNC211 (UvrB), and pDR3274 (UvrC) [45]. The methods of purification were the same as described previously [46]. For the experiments using the DNA fragments from the pCAT and pBR322 plasmids, the UvrABC proteins were purchased from PharMingen (San Diego, CA, USA).

5.6. DNA fragment isolation and ^{32}P-end-labeling

Plasmid pGEM inserted with APRT gene from Chinese hamster ovary cells was purified via cesium chloride density centrifugation and dialyzed extensively against TE buffer. The 284-bp fragment of exon III of the APRT gene was obtained by digesting plasmid DNA with restriction enzymes *Pst*I and *Stu*I. The band corresponding to the 284-bp fragment was isolated from 1.4% agarose gel and cleaned by passing through a NACS Prepac column followed by ethanol precipitation. The 284-bp fragment was further cut with the restriction enzyme *Mse*I to generate a 188-bp fragment with a unique site for a single 3′-end-labeling. DNA labeling was accomplished in the presence of [α-^{32}P]TTP and Klenow fragment (5 U) in 10 mM Tris–HCl (pH 8.0), 5 mM $MgCl_2$, and 7.5 mM dithiothreitol (DTT) at 22°C. The 3′-end-labeled fragment was purified on a 5% polyacrylamide gel. For 5′-end-labeling, the restriction enzyme *Hin*fI was used to cut the 284-bp fragment to create protruding 5′ termini. The resulting fragment was treated with bacterial alkaline phosphatase at 60°C for 1 h. The dephosphorylated fragment was extracted with phenol–chloroform and purified by gel electrophoresis. The purified fragment was then labeled with [γ-^{32}P]ATP in the presence of T4 polynucleotide kinase. The labeled fragment was precipitated with ethanol and digested with *Mse*I to afford a 170-bp 5′-end-labeled fragment, which was then isolated and purified as above.

For the isolation of a 209-bp fragment labeled at the 5′-end with ^{32}P, the pCAT plasmid (New England Biolabs) was first digested with *Hin*dIII followed by treatment with shrimp alkaline phosphatase at 37°C for 2 h. The dephosphorylated fragment was extracted with phenol–chloroform and then ethanol-precipitated. The precipitated DNA was labeled with [γ-^{32}P]ATP in the presence of T4 polynucleotide kinase. The labeled DNA was then incubated with *Eco*RI and gel-purified to yield the 209-bp 5′-end-labeled fragment. For 3′-end-labeling, the restriction enzyme *Eco*RI was used to cut the pCAT plasmid. DNA labeling was accomplished in the presence of [α-^{32}P]ATP and Klenow fragment. The 3′-end-labeled DNA was then incubated with *Hin*dIII and purified on a 6% polyacrylamide gel. The same protocol was used to generate a 200-bp fragment from the pBR322 plasmid (New England Biolabs) except the restriction enzymes *Nhe*I and *Bam*HI were used.

5.7. Construction of the Et 743–DNA adducts

The 22-bp duplex DNA [(5′-TGGTTATATAAGCTATTA-TAAT-3′)(3′-ATATATTCGATAATATTAGCTC-5′)] containing a single 5′-AGC alkylation site was modified with 20 μM Et 743 for 2 h. Unreacted drug was removed by phenol–chloroform extraction followed by ethanol precipitation. The Et 743-modified DNA was ligated to a radiolabeled duplex DNA, on either the 5′- or 3′-side, by incubating with T4 DNA ligase (1 U/100 μl) at 16°C for 12 h. After gel purification, the resulting Et 743-modified duplex was ligated to another duplex, on either the 3′- or 5′-side of the modified DNA fragment. The site-directed adduct was gel-purified and eluted in annealing buffer.

5.8. UvrABC nuclease reactions

The UvrABC nuclease reactions were carried out in a reaction mixture (30 μl) containing 50 mM Tris–HCl (pH 7.5), 0.1 mM EDTA, 10 mM $MgCl_2$, 1 mM ATP, 100 mM KCl, 1 mM DTT, 60 nM UvrA, 120 nM UvrB, 60 nM UvrC, and substrate DNA. The mixtures were incubated at 37°C for 1 h and the reactions were stopped by phenol–chloroform extraction followed by ethanol precipitation in the presence of aqueous ammonium acetate (2.5 M). The precipitated DNA was recovered by centrifugation and washed with 80% ethanol.

For the DNA fragments isolated from the pCAT and pBR322 plasmids, the UvrABC nuclease reactions were carried out in a reaction mixture (20 μl) containing 50 mM Tris–HCl (pH 7.5), 10 mM $MgCl_2$, 2 mM ATP, 50 mM KCl, 5 mM DTT, 0.1 mg/ml bovine serum albumin, 10 nM UvrA, 80 nM UvrB, 12 nM UvrC, and substrate DNA. The mixtures were incubated at 37°C for 1 h and then precipitated with ethanol. The samples were loaded on an 8% denaturing sequencing gel.

6. Note added in proof

In the recently published paper by Takebayashi et al. [23], there is demonstration of accumulation of DNA single-strand breaks in transcription-coupled (TC) NER-proficient fibroblasts treated with Et 743. Thus, our observation of a low frequency of uncoupled 3′ or 5′ incisions may be of significance. The conclusion in this paper that 'trapping of the TC-NER complex stalled [during or] after DNA cleavage' is exactly in accord with our results and conclusions. This finding is similar to that reported for phleomycin [47], anthramycin [25], and ditercalinium [48].

Acknowledgements

This research was supported by Grants from the National Institutes of Health (CA49751 and CA29756). The American Chemical Society Division of Medicinal Chemistry and Hoechst Marion Roussel are gratefully acknowledged for support of a predoctoral fellowship awarded to M.Z.-F. We thank Professor M.-s. Tang (New York University) for the DNA fragment from the APRT gene and the UvrABC proteins used in the experiments shown in Fig. 4A,B. We are grateful to Dr. Bennett Van Houten (NIEHS) for insightful discussions. We thank Dr. David Bishop for preparing, proofreading, and editing the final version of the manuscript and figures.

References

[1] K.L. Rinehart, T.G. Holt, N.L. Fregeau, J.G. Stroh, P.A. Keifer, F. Sun, L.H. Li, D.G. Martin, Ecteinascidins 729, 743, 745, 759A, 759B, and 770: potent antitumor agents from the Caribbean tunicate *Ecteinascidia turbinate*, J. Org. Chem. 55 (2000) 4512–4515.

[2] J.M. Jimeno, G. Faircloth, L. Cameron, K. Meely, E. Vega, A. Gomez, J.M.F. Sousa-Faro, K. Rinehart, Progress in the acquisition of new marine-derived anticancer compounds: development of the ecteinascidin-743 (Et-743), Drugs Future 21 (1996) 1155–1165.

[3] R. Sakai, E.A. Jares-Erijman, I. Manzanares, M.V. SilvaElipe, K.L. Rinehart, Ecteinascidins: putative biosynthetic precursors and absolute stereochemistry, J. Am. Chem. Soc. 118 (1996) 9017–9023.

[4] A. Bowman, C. Twelves, K. Hoekman, A. Simpson, J. Smyth, J. Vermorken, F. Hoppener, J. Beijnen, E. Vega, J. Jimeno, A.-R. Hanauske, Phase I clinical and pharmacokinetic (PK) study of ecteinascidin-743 (Et-743) given as a one hour infusion every 21 days, Ann. Oncol. 9 (Suppl. 2) (1998) 119.

[5] M. Villalona-Calero, S.G. Eckhardt, G. Weiss, E. Campbell, M. Hidalgo, M. Kraynak, J. Beijnen, J. Jimeno, D. Von Hoff, E. Rowinsky, A phase I and pharmacokinetic study of ET-743, a novel DNA minor groove binder of marine origin, administered as a 1-hour infusion daily $\times 5$ days, Ann. Oncol. 9 (Suppl. 2) (1998) 119.

[6] A. Taamma, J.L. Misset, M. Riofrio, C. Guzman, E. Brain, L. Lopez Lazaro, H. Rosing, J.M. Jimeno, E. Cvitkovic, Phase I and pharmacokinetic study of ecteinascidin-743, a new marine compound, administered as a 24-hour continuous infusion in patients with solid tumors, J. Clin. Oncol. 19 (2001) 1256–1265.

[7] G.C. Hill, W.A. Remers, Computer simulation of the binding of saframycin A to $d(GATGCATC)_2$, J. Med. Chem. 34 (1991) 1990–1998.

[8] K. Rao, J. Lown, Mode of action of saframycin antitumor antibiotics: sequence selectivities in the covalent binding of saframycins A and S to deoxyribonucleic acid, Chem. Res. Toxicol. 3 (1990) 262–267.

[9] K. Rao, J. Lown, DNA sequence selectivities in the covalent bonding of antibiotic saframycins Mx1, Mx3, A, and S deduced from MPE·Fe(II) footprinting and exonuclease III stop assays, Biochemistry 31 (1992) 12076–12082.

[10] M.J. Zmijewski Jr., K. Miller-Hatch, M. Mikolajczak, The in vitro interaction of naphthyridinomycin with deoxyribonucleic acids, Chem. Biol. Interact. 52 (1985) 361–375.

[11] L.H. Hurley, R. Petrusek, Proposed structure of the anthramycin–DNA adduct, Nature 282 (1979) 529.

[12] B.M. Moore II, F.C. Seaman, L.H. Hurley, NMR-based model of an ecteinascidin 743–DNA adduct, J. Am. Chem. Soc. 119 (1997) 5475–5476.

[13] Y. Pommier, G. Kohlhagen, C. Bailly, M. Waring, A. Mazumder, K.W. Kohn, DNA sequence- and structure-selective alkylation of guanine N2 in the DNA minor groove by ecteinascidin 743, a potent antitumor compound from the Caribbean tunicate *Ecteinascidia turbinate*, Biochemistry 35 (1996) 13303–13309.

[14] B.M. Moore II, F.C. Seaman, R.T. Wheelhouse, L.H. Hurley, Mechanism for the catalytic activation of ecteinascidin 743 and its subsequent alkylation of guanine N2, J. Am. Chem. Soc. 120 (1998) 2490–2491.

[15] F.C. Seaman, L.H. Hurley, Molecular basis for the DNA sequence selectivity of ecteinascidin 736 and 743: evidence for the dominant role of direct readout via hydrogen bonding, J. Am. Chem. Soc. 120 (1998) 13028–13041.

[16] M. Zewail-Foote, L.H. Hurley, Differential rates of reversibility of ecteinascidin 743–DNA covalent adducts from different sequences lead to migration to favored bonding sites, J. Am. Chem. Soc. 123 (2001) 6485–6495.

[17] E. Cvitkovic, M. Riofrio, F. Goldwasser, S. Delaloge, A. Taamma, J. Beijnen, J.M. Jimeno, B. Mekranter, C. Guzman, E. Brain, J.L. Misset, Final results of phase I study of ecteinascidin-743 (Et-743) 24 hour continuous infusion (CI) in advanced solid tumors (AST) patients, Proc. ASCO 18 (1999) 180a.

[18] D.P. Ryan, J.G. Supko, J.P. Eder, H. Lu, B. Chabner, K. Roper, P. Baccala, J. Bonenfant, G. Faircloth, C. Guzman, J. Jimeno, J.W. Clark, A phase I and pharmacokinetic trial of ecteinascidin-743 (Et-743) administered as a 72 hour continuous infusion, Proc. ASCO 18 (1999) 188a.

[19] M. Zewail-Foote, L.H. Hurley, Ecteinascidin 743: a minor groove alkylator that bends DNA toward the major groove, J. Med. Chem. 42 (1999) 2493–2497.

[20] E.J. Martinez, T. Owa, S.L. Schreiber, E.J. Corey, Phthalascidin, a synthetic antitumor agent with potency and mode of action comparable to ecteinascidin 743, Proc. Natl. Acad. Sci. USA 96 (1999) 3496–3501.

[21] Y. Takebayashi, P. Pourquier, A. Yoshida, G. Kohlhagen, Y. Pommier, Poisoning of human DNA topoisomerase I by ecteinascidin 743, an anticancer drug that selectively alkylates DNA in the minor groove, Proc. Natl. Acad. Sci. USA 96 (1999) 7196–7210.

[22] S. Jin, B. Gorfajn, G. Faircloth, K. Scotto, Ecteinascidin 743, a transcription-targeted chemotherapeutic that inhibits MDR1 activation, Proc. Natl. Acad. Sci. USA 97 (2000) 6775–6779.

[23] Y. Takebayashi, P. Pourquier, D.B. Zimonjic, K. Nakayama, S. Emmert, T. Ueda, Y. Urasaki, A. Kanzaki, S. Akiyama, N. Popescu, K.H. Kraemer, Y. Pommier, Antiproliferative activity of ecteinascidin 743 is dependent upon transcription-coupled nucleotide-excision repair, Nature Med. 7 (2001) 961–966.

[24] G. Damia, S. Silvestri, L. Filiberti, M. Broggini, M. D'Incalci, Importance of DNA repair mechanisms for the sensitivity of tumor cells to ET-743, Proceedings of the 1999 AACR-NCI-EORTC International Conference on Molecular Targets and Cancer Therapeutics, 1999, p. 3872.

[25] R.L. Petrusek, E.L. Uhlenhopp, N. Duteau, L.H. Hurley, Reaction of anthramycin with DNA. Biological consequences of DNA damage in normal and *Xeroderma pigmentosum* cell lines, J. Biol. Chem. 257 (1982) 6207–6216.

[26] A. Sancar, DNA excision repair, Annu. Rev. Biochem. 65 (1996) 43–81.

[27] B. Van Houten, A. McCullough, Nucleotide excision repair in *E. coli*, Ann. N.Y. Acad. Sci. 726 (1994) 236–251.

[28] T. Lindahl, R.D. Wood, Quality control by DNA repair, Science 286 (1999) 1897–1905.

[29] H. Kohn, V.-S. Li, M.-s. Tang, Recognition of mitomycin C–DNA monoadducts by UvrABC nuclease, J. Am. Chem. Soc. 114 (1992) 5501–5509.

[30] R.B. Walter, J. Pierce, R. Case, M.-s. Tang, Recognition of the DNA helix stabilizing anthramycin–N2 guanine adduct by UvrABC nuclease, J. Mol. Biol. 230 (1988) 939–947.

[31] C.P. Selby, A. Sancar, ABC excinuclease incises both 5′ and 3′ to the CC-1065–DNA adduct and its incision activity is stimulated by DNA helicase II and DNA polymerase I, Biochemistry 27 (1988) 7184–7188.

[32] R. Visse, M. de Ruijter, J. Brouwer, J.A. Brandsma, P. van de Putte, Uvr excision repair protein complex of *Escherichia coli* binds to the convex side of a cisplatin-induced kink in the DNA, J. Biol. Chem. 266 (1991) 7609–7617.

[33] D.K. Orren, A. Sancar, The (A)BC excinuclease of *Escherichia coli* has only the UvrB and UvrC subunits in the incision complex, Proc. Natl. Acad. Sci. USA 86 (1989) 5237–5241.

[34] D.K. Orren, A. Sancar, Formation and enzymatic properties of the UvrB–DNA complex, J. Biol. Chem. 265 (1990) 15796–15803.

[35] Y. Zou, B. Van Houten, Strand opening by the $UvrA_2B$ complex allows dynamic recognition of DNA damage, EMBO J. 18 (1999) 4889–4901.

[36] K. Theis, P.J. Chen, M. Skorvaga, B. Van Houten, C. Kisker, Crystal structure of UvrB, a DNA helicase adapted for nucleotide excision repair, EMBO J. 18 (1999) 6899–6907.

[37] J.J. Lin, A.M. Phillips, J.E. Hearst, A. Sancar, Active site of (A)BC excinuclease. II. Binding, bending, and catalysis mutants of UvrB reveal a direct role in 3′ and an indirect role in 5′ incision, J. Biol. Chem. 267 (1992) 17693–17700.

[38] R. Visse, A. King, G.F. Moolenaar, N. Goosen, P. van de Putte, Protein–DNA interactions and alterations in the DNA structure upon UvrB–DNA preincision complex formation during nucleotide excision repair in *Escherichia coli*, Biochemistry 33 (1994) 9881–9888.

[39] E.Y. Oh, L. Grossman, The effect of *Escherichia coli* Uvr protein binding on the topology of supercoiled DNA, Nucleic Acids Res. 14 (1986) 8557–8571.

[40] Q. Shi, R. Thresher, A. Sancar, J. Griffith, Electron microscopic study of (A)BC excinuclease. DNA is sharply bent in the UvrB–DNA complex, J. Mol. Biol. 226 (1992) 425–432.

[41] G.F. Moolenaar, K.L.M.C. Franken, D.M. Dijkstra, J.E. Thomas-Oates, R. Visse, P. van de Putte, N. Goosen, The C-terminal region of the UvrB protein of *Escherichia coli* contains an important determinant for UvrC binding to the pre-incision complex but not the catalytic site for 3′ incision, J. Biol. Chem. 270 (1995) 30508–30515.

[42] Y. Zou, T.M. Liu, N.E. Geacintov, B. Van Houten, Interaction of the UvrABC nuclease system with a DNA duplex containing a single stereoisomer of dG-(+)- or dG-(−)-anti-BPDE, Biochemistry 34 (1995) 13582–13593.

[43] J.-J. Lin, A. Sancar, Active site of (A)BC excinuclease. I. Evidence for 5′ incision by UvrC through a catalytic site involving Asp^{399}, Asp^{438}, Asp^{466}, and His^{538} residues, J. Biol. Chem. 267 (1992) 17688–17692.

[44] E.E.A. Verhoeven, M. van Kesteren, G.F. Moolenaar, R. Visse, N. Goosen, Catalytic sites for 3′ and 5′ incision of *Escherichia coli* nucleotide excision repair are both located in UvrC, J. Biol. Chem. 275 (2000) 5120–5123.

[45] D.C. Thomas, M. Levy, A. Sancar, Amplification and purification of UvrA, UvrB, and UvrC proteins of *Escherichia coli*, J. Biol. Chem. 260 (1985) 9875–9883.

[46] M.-S. Tang, Mapping and quantification of bulky chemical-induced DNA damage using UvrABC nucleases, in: G.P. Pfeifer (Ed.), Technologies for Detection of DNA Damage and Mutations, Plenum Press, New York, 1996, pp. 139–153.

[47] E. Schrock, S. du Manoir, T. Veldman, B. Schoell, J. Wienberg, M.A. Ferguson-Smith, Y. Ning, D.H. Ledbetter, I. Bar-Am, D. Soenksen, Y. Garini, T. Ried, Multicolor spectral karyotyping of human chromosomes, Science 273 (1996) 494–497.

[48] B. Lambert, B.P. Roques, J.B. Le Pecq, Induction of an abortive and futile DNA repair process in *E. coli* by the antitumor DNA bifunctional intercalator, ditercalinium: Role in polA in death induction, Nucleic Acids Res. 16 (1988) 1063–1078.